



INSTITUT DE FRANCE
Académie des sciences

Comptes Rendus

Chimie

Latifa Morjène, Fadhel Aloulou and Mongi Seffen

Effect of organoclay and wood fiber inclusion on the mechanical properties and thermal conductivity of cement-based mortars

Volume 23, issue 11-12 (2020), p. 733-746


Published online: 3 February 2021

Issue date: 3 February 2021

<https://doi.org/10.5802/crchim.42>

Part of Special Issue: Sustainable Biomass Resources for Environmental, Agronomic, Biomaterials and Energy Applications 1

Guest editors: Mejdi Jeguirim (Institut de Science des Matériaux de Mulhouse, France), Salah Jellali (Sultan Qaboos University, Oman) and Bisma Khiari (Water Research and Technologies Centre, Tunisia)

 This article is licensed under the
CREATIVE COMMONS ATTRIBUTION 4.0 INTERNATIONAL LICENSE.
<http://creativecommons.org/licenses/by/4.0/>



*Les Comptes Rendus. Chimie sont membres du
Centre Mersenne pour l'édition scientifique ouverte*

www.centre-mersenne.org

e-ISSN : 1878-1543



Sustainable Biomass Resources for Environmental, Agronomic, Biomaterials and Energy Applications 1 / *Ressources de biomasse durables pour des applications environnementales, agronomiques, de biomatériaux et énergétiques 1*

Effect of organoclay and wood fiber inclusion on the mechanical properties and thermal conductivity of cement-based mortars

Latifa Morjène^a, Fadhel Aloulou^{*, a} and Mongi Seffen^a

^a Laboratory of Energy and Materials: LabEM-LR11ES34, University of Sousse, Tunisia

E-mails: morjene.latifa@gmail.com (L. Morjène), alouloufadhel@gmail.com (F. Aloulou), mongiseffen@yahoo.fr (M. Seffen)

Abstract. Nowadays, there is an enormous demand for constructing housing that needs to be catered for a short span of time, with minimum transportation costs and in an ecological manner. Biobased materials are considered to be a promising resource for buildings in the twenty-first century due to their sustainability and versatility. This article discusses biopositive materials and low-cost renewable “green” technologies that are used in low-rise multi-functional architecture. It explores the use of organic clay (OC) and wood fibers treated with NaOH (WFsT) as reinforcement materials in cement mortars. The compressive strength, porosity, hydration rate and thermal conductivity of different formulations of reinforced cement were recorded. It was found that the best dispersion and the stabilization of WFsT in the composite materials are achieved with the addition of 6% WFsT in the presence of an anionic surfactant sodium dodecylbenzene sulfonate (SDBS). The results revealed that the optimal composite material was a mix of water with Ordinary Portland Cement (OPC) and 1 wt% modified with Cetyltrimethylammonium bromide (CTAB) at a water-to-solid ratio of 0.65. With OC contents from 2% up to 18%, compressive strength results were higher than that of the plain cement paste and a decrease of the thermal conductivity was obtained by the addition of 2 wt% of WF from 2.26 to 0.8 W/m·°C. The presence of WFsT influenced the hydration of the cement while promoting the formation of more portlandite and more calcium silicate gel.

Keywords. Composite, Compressive strength, Thermal conductivity, Organoclay, Natural clay, Wood fibers.

1. Introduction

The choices of materials used in constructions are of high importance. Cementitious building materials reinforced with vegetable fibers are the biomateri-

als needed for construction and building. This composite enhances the mechanical performance among other properties.

Clay-based composite along with natural fibers are being tested as cementitious composites in the building sector [1–4].

These formulations are aimed to help developing

* Corresponding author.

cost-effective ecofriendly construction materials.

However, the stake of this composite formation is the cracks caused to the cement mortar, the weak interaction between natural fibers, organoclay (OC) and the cement matrix and the decline of the building thermal properties. As a solution, it is useful to incorporate several types of nanoparticles into the cement, ceramic and polymer matrixes of the building material in order to produce nanocomposites [5,6] with good mechanical and thermal conductivity properties. Several types of nanoparticles were used in the literature; e.g., TiO₂ [7], ZnO [8] and OC [9].

In recent studies, and in order to improve the quality, sustainability and cost of cement cellulose fibers have been extracted from several sources such as jute fibers [10], cellulosic fibers [11] and natural clay [12, 13]. The incorporation of these traditional fibers in polymer-based composite materials was aimed to enhance and to improve their mechanical flexibility as well as their thermal insulation [5].

Composites have been found to be the most promising material available nowadays.

Recently, several studies have focused on the dispersion and stability of cellulose nanofibers as reinforcing materials in a cement matrix.

These studies have shown that the addition of cellulose fibers (from 1 wt% to 5 wt%) enhances the bending strength up to 100% and the absorption energy of the cement up to 150% [14].

Other studies proved that the addition of cellulose (CNC) improves the flexural strength, specifically the resistance to bending due to the increase in hydration of cement pastes with the cellulose nanocrystals [6].

More recently, studies on the effect of date palm fibers added in cement-based formulations showed that the mechanical and thermal insulation properties were increased up to 52% in thermal properties.

Biobased materials of natural and OC [15] sources were used to reinforce cement, improve the mechanical properties and strength of cementitious materials and accelerate the formation and the precipitation of hydration [16,17]. Clay, who belongs to the group of phyllosilicates, could also replace other fibers in many applications. This material is considered to have a wide range of applications [8,9]. Modified clays such as chlorite, natural clay and Illite, are used as fillers in the composite material that enhance

the cement properties. Results showed that the modified OC has enhanced the adhesion of fiber/clay inside the cement materials. Thus, the mechanical and thermal properties of the cement nanocomposites were improved. Modification of mineral clay is a necessity to obtain a homogenous material.

These clays have the merits of low cost, availability and excellent characteristics [18]. These fibers are also praised for being biodegradable, light-weight and abundant resources [19].

The industrial application of OC has been recognized in the literature due to the excellent performance that engendered on the physical properties of the elaborated composites [3,11,13,20]. Several obstacles are encountered which limit the application of natural fiber in cement composites [15]. One can cite several causes. First the interfacial bond existing between the fiber and the cement matrix is relatively weak. Second, the degradation of the fibers in a high alkaline cement adversely affects the mechanical properties and durability of such reinforced composites [16].

In this work, the wood fiber (WF) and OC supplementation in the cement matrix was aimed to improve the mechanical resistance and the microstructural characteristics of the matrix by strengthening the bonding existing between the matrix and the WFsT [17] and to reduce the alkalinity of the matrix.

2. Methods

2.1. Description of used materials

Ordinary Portland cement (OPC NF P 15-301) was used in all the cement formulation. More information about the chemical composition of OPC [21] is presented in Table 1.

Wood Fibers (abbreviated as WFsT) used in this study are chemically treated by following a TAAPI method in which the individual components (e.g., cellulose, hemicellulose and lignin) are separated and quantitatively determined (Table 2), [22].

The clay platelets used in this work were natural clay from Jemmel city (Tunisia).

The CTAB is a cationic surfactant (Mw 336.39 g·mol⁻¹), a quaternary alkyl ammonium salt soluble in H₂O and used in the preparation of OC. The SDBS (Mw 348.48 g·mol⁻¹) is sodium

Table 1. Constituents of Ordinary Portland cement [21]

Oxides	Cement (wt%)
CaO	65.47
SiO ₂	19.82
Al ₂ O ₃	4.66
Fe ₂ O ₃	3.03
CaO	65.47
MgO	0.84
K ₂ O	0.64
Na ₂ O	0.10
TiO ₂	0.16
SO ₃	2.87
Loss ignition(LOI)	3.5
Density	3.2 g/cm ³
Surface area	355 m ² /kg
Particle size	18.54 μm

dodecylbenzene sulfonate, an anionic surfactant used in the fabrication of composites.

The chemical composition of WFs is listed in Table 2.

2.2. Chemical treatment

2.2.1. Treatment of wood fibers

A mass of 5 g of the WFs were placed in 100 mL of aqueous solution of hydroxide (NaOH: 1 M) Sigma-Aldrich (98%), at pH = 12 for 1 h at 80 °C. They were then washed with distilled water. Finally, WFs with a diameter of <40 μm, from Hammam Sousse, Tunisia [23], were dried in the oven at 80 °C for one day. The treatment of WFs enhances the homogeneity between C-WFsT-OC, which improves the mechanical properties of the matrix.

2.2.2. Treatment of natural clay

The natural clay was washed with distilled water to eliminate impurities. Then, the clay was attacked with sulfuric acid (2 M), and 500 g of clay was dispersed in 1 L of distilled water under stirring at 80 °C until complete dispersion. The solution was kept during 24h. After this time, the clay was washed three times with distilled water and filtered until a pH value of 7. At the end, the clay was treated with CTAB

Table 2. Chemical composition of wood fibers [22]

Cellulosic residue (wt%)	Hemicellulose (wt%)	Lignin (wt%)	(Pectin) (wt%)
Wo wood fiber 40–50	25–40	15–35	1–8

and washed with distilled water following the same procedure applied with sulfuric acid.

2.2.3. Preparation of organoclay (OC)

To obtain organophilic clays, pure clay was modified with CTAB for 3 h. In this context, different studies have shown that this surfactant [24] intercalation can change the hydrophilic character of the natural clay surface and increase the clay interlayer basal spacing.

The treatment of clay started by introducing 10 ml of hydrochloric acid (1 M). Then, this solution is heated to 80 °C. Then, we put 10 m moles of CTAB, for 3 h of stirring in 80 °C, and 10 g of clay was added. Finally, after 3 h of cationic exchange, the clay is filtered to eliminate the inorganic cations. At the end, the clay is dried at 80 °C.

2.3. Preparation of composites

Samples contained OPC alone or OPC-OC-WF with different formulations, with a water/OC-Cement ratio equal to 0.65. OPC and OC were slowly mixed for 5 min until homogenization.

Specimens with dimensions of 3.5 × 7 × 1.75 (cm) were cast in the mechanical tests. The mix proportions are illustrated in Table 3. After 24 h, all samples were unmolded and immersed in water for 28 days. Bend experiment was controlled using an “MTS Insight” to examine the compressive strength. The compressive strength results are the average of the three test values.

The compositions of mixtures made with different rates of WFsT and OC that were used in the thermal conductivity and compressive strength tests are given in Table 3.

2.4. Physical properties

In order to define the quality of composite samples, different measurements of porosity and density were conducted following the ASTM standard (C-20) [25].

Table 3. Mixture formulations

Composite recipes	Cement (%)	Wood fibers	Organoclay	W/C
Cement	115	-	-	0.5
C+WFsNT	99	6	-	0.6
C+ WFsT	114	1	-	0.65
	113	2	-	0.65
	111	4	-	0.65
	99	6	-	0.65
	97	8	-	0.65
	95	10	-	0.65
	C+WFsT+OC	98.5	6	0.5
98		6	1	0.65
97.5		6	0.5	0.65

C: Cement; WFsNT: Wood Fibers Non-Treated; WFsT: Wood Fibers Treated; W: Water.

With the ethanol displacement method, the porosity of composites was evaluated. Ethanol can be adsorbed into the microstructure of composites without fissuration and cracks. After 28 days of curing, samples were crushed into particles and were immersed in ethanol. After that, these particles were dried at 40 °C until obtaining a constant weight. Then, they were placed in ethanol solution for 24 h, and the mass of samples immersed in ethanol was named m_i . The particles were then dried. Finally, the measurement mass was named m_s .

Measurement of porosity (P_s) was determined using the following Eq (1) [26]:

$$P_s\% = (m_s - m_d)/(m_s - m_i) \quad (1)$$

m_i = mass of the sample saturated in ethanol.

m_s = mass of the sample saturated in air.

m_d = mass of the specimen dried (g).

In order to determine the bulk density, different parameters such as length, thickness, mass and width were determined by using Eq (2) [26]:

$$D = m_d / V, \quad (2)$$

where D is the density (g/cm^3), m_d is the oven dried weight (g) and V is the volume of the test sample (cm^3).

2.5. Characterization

The WFsT modified were characterized via Fourier transform infrared spectroscopy (FTIR). Further-

more, OC in powder form was characterized via structure X-ray diffraction. The effect of OC prepared by treating clay with Cetyltrimethyl ammonium bromide (CTAB) on the physical and mechanical properties of WF-reinforced composites was also investigated.

2.5.1. X-ray diffraction (XRD)

The XRD pattern was measured with an X-ray Diffractometer in the 2θ range between 9° and 60° , using $\text{CuK}\alpha$ ($\gamma = 1.54060 \text{ \AA}$) radiation at 40 KV and 30 mA. With an exceptional analysis speed, with a step size of $0.02^\circ/\text{s}$ a collection time of 40 s per step and an incident angle of 1° . The crystallization degree is obtained by comparing the intensity of the crystalline and the amorphous curve.

The crystalline degree of OC was calculated from an XRD profile. X-ray measurements were made on sample sheets pushed in powder after the air-drying of the OC.

2.5.2. Fourier transform infrared spectroscopy (FTIR)

Fourier transform infrared spectroscopy (FTIR) using a Perkin Elmer spectrometer (spectrum two, from 2011) with a resolution of 2 cm^{-1} in the range of $400\text{--}4000 \text{ cm}^{-1}$ served to analyze the change of functional groups at the WFs and the natural clay after treatments with NaOH, sulfuric acid and CTAB, respectively. All FTIR measurements were done in transmittance mode after baseline correction. The

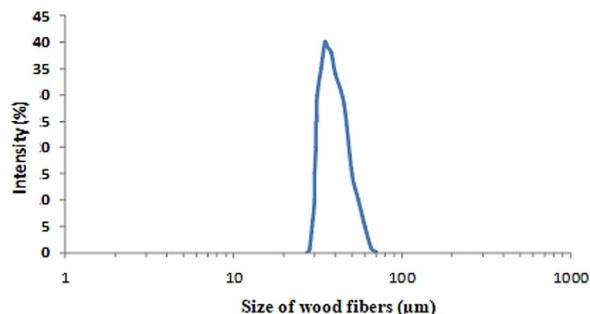


Figure 1. Size of wood fibers.

method is very classic, the sample is ground with transparent potassium bromide (KBr) then is pressed in pellet form to perform IR spectra analyzes.

2.5.3. Contact angle measurements

Contact angle is measured to study the capacity of a liquid spread out on a surface by wet ability. In this work, this technique was used to evaluate the hydrophilicity (small angle)/hydrophobicity (energy of the surface) character, to analyze the aspect of the composite surface, and to study the effect of WFs treated with NaOH and of SDBS on the absorbability of water. Contact angle measurements were modulated by using a goniometry coupled to an image analysis program. For the measurement of the contact angle, drops of calibrated distilled water were deposited on the pellets of modified cellulosic fibers. The contact angle device used was an OCA 15 from Dataphysics, equipped with a CCD camera, with a resolution of 752×582 square pixels, operating at an acquisition rate of 4 images per second. The data collected was processed using OCA software [27].

2.6. Thermal conductivity measurements

The thermal conductivity of composite samples of dimensions ($24.5 \times 1.5 \times 24.5$ cm) was measured after 28 days of treatment using a “Heat Transmission Study Bench—PTC 100.”

3. Results and discussion

3.1. Particle size determination of wood fibers

The WFsT (Figure 1) were in a distribution of monomodal size, which were narrow (PDI) around $0.2 \mu\text{m}$ with a diameter of $<40 \mu\text{m}$.

The particle size diameters of WFsT and their hydrodynamic diameters were measured at 20°C using a Malvern Nano-zetasizer ZS (Malvern, UK) with a fixed scattering angle of 173° . The dispersions were not diluted before starting the measurements [22]. Dynamic light scattering measurements gave an Z-average size that was used for comparison of the different particles.

3.2. XRD

3.2.1. Organoclay

The XRD patterns of natural clay and natural clay modified with the CTAB are shown in Figures 2a and b. Figure 2a shows the presence of pure natural clay characteristic peaks at specific reflection $2\theta = 6.4^\circ$ (d_{001}) and 19.83° (d_{020}). The natural clay was identified by XRD measurement evidencing the characteristic diffraction peaks of quartz (26.9°) and Kaolinite (22.1°). These peaks refer to the presence of natural clay. Compared to other works, the peak at $2\theta = 37.55^\circ$ and 38.02° corresponds to natural clay [28]. Typical XRD patterns of natural clay, after the treatment with the CTAB show diffraction peaks at 5.13° . This result was due to the linear structure of CTAB (19 carbons) and reveals the existence of a smectite, which affirms that this clay belongs to the natural clay family. The CTAB natural clay matrix has a highest value of the interfoliar space $d_{020} = 19.83 \text{ \AA}$ corresponding to the inter planar spacing [29]. From Figure 2, the (001) reflection, as it had shifted from $2\theta = 6.4^\circ$ corresponding to the spacing increasing from $d_{001} = 0.83$ to 1.23 nm , confirms that the CTAB surfactant has been interlayered between the layers of the pure natural clay. This result was accomplished by comparison with other researches using TiO_2 and not CTAB [30]. Added to these results, the reflection 001 is related to the number of mineral layers and the mode of stacking [31,32].

To explain the influence of WFsT, the phase composition of cement was determined through XRD of cement with a percentage variation of WFsT [27]. The corresponding XRD patterns, at one day of treatment, are shown in Figure 3. The XRD of the three composites show the hydration products, including portlandite, ettringite and unreacted calcium silicate phases (C_3S and C_2S). Moreover, as the calcium-silicate-hydrates (C-S-H gel) were poorly crystallized, in the patterns spectra, diffraction peaks could

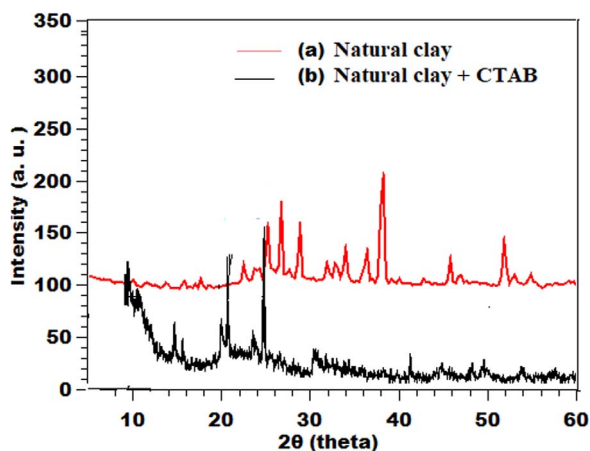


Figure 2. XRD pattern of (a) natural clay and (b) natural clay with CTAB.

be clearly viewed. In addition, the evolution of C–S–H gel is evaluated referring to the unreacted anhydrous cement phases. The intensity of calcium silicate main peaks were reduced with WFsT supplementation, as a greater amount of anhydrous cement phases reacted in the presence of WFsT (C_3S and C_2S are transformed into C–S–H). Besides, higher amounts of portlandite and ettringite were formed in WFsT 1% and WFsT 2% samples, compared to the control paste WFsT 0%. The intensity of peak changes continued to increase as a function of WFsT. Compared to the pure cement sample, it can be confirmed that the presence of WFsT promotes the early hydration of cement by producing more portlandite, ettringite and C–S–H gel. As C–S–H is one of the major hydration products and the main binding phases in Portland cement controlling cement mechanical properties, the higher content in C–S–H phase is likely the main reason accounting for the strong enhancement in the compressive strength of the cement matrix.

3.3. FTIR spectroscopy

3.3.1. Infrared spectral characteristics of wood fibers

The FTIR spectra in the range $4000\text{--}500\text{ cm}^{-1}$ of different samples are shown in Figure 4. The main characteristic bands of WFsT before and after treatment are listed as follows:

The presence of a large band at 3386 cm^{-1} corresponds to hydroxyl group characteristic of polysaccharides [33].

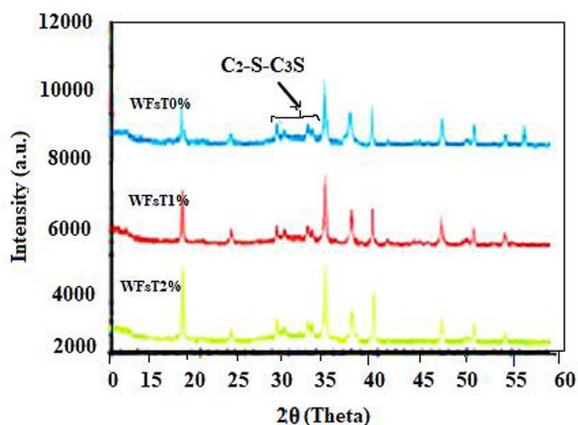


Figure 3. XRD spectra of the WFsT 0%, WFsT 1% and WFsT 2% at one curing day.

The bands at 2930 and 2898 cm^{-1} are due successively to sym and asym CH_2 in polysaccharides and fats [34]. The FTIR spectrum exhibits the presence of two carbonyl and acetyl groups existing in the xylan component ($C=O$ stretching vibration) at 1732 cm^{-1} . However, this peak almost disappears when these fibers are treated with 2% NaOH.

The peak around 1635 cm^{-1} corresponds to stretching vibration of the hydroxyl group and characteristic to water molecules. Furthermore, the peak at 1436 cm^{-1} is assigned to the asymmetric CH deformation in lignin and hemicellulose structures.

Concerning the FTIR of non-treated WFsT, the band at 1512 cm^{-1} confirms the presence of lignin and is due to the aromatic skeletal vibration ($C=C$). In the spectrum of WFsT treated 5% NaOH, the elimination of lignin after NaOH treatment confirmed the decrease of large band (1512 cm^{-1}). The small peaks at 1375 cm^{-1} in the spectrum of non-treated WFsT, WFsT treated 0.5%, 2% are related to CH_2 vibration. In all the FTIR spectra, the band at 1168 cm^{-1} is assigned to the hemicelluloses and lignin corresponding to the C–O–C asymmetric stretching.

The peak at 1042 cm^{-1} is assigned to lignin or hemicelluloses (C–O–C linkage) [25]. The presence of CH rock vibrations band at 810 cm^{-1} is attributed to the presence of cellulose.

Alkaline treatment is relatively conventional. Figure 4 shows the effect of NaOH on the fibers. A certain amount of lignin, wax and impurities was eliminated. Thus treatment promotes lignin extraction and partial degradation of hemicelluloses. It is noted that

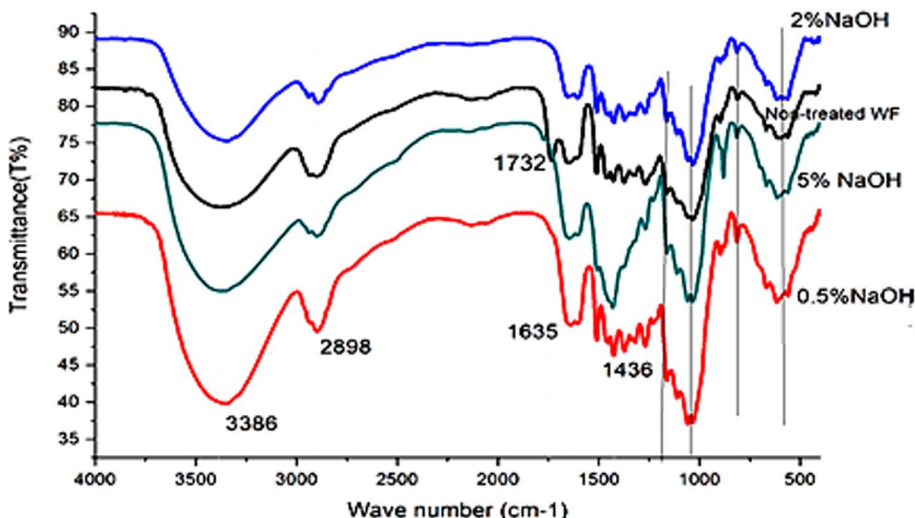


Figure 4. FTIR spectra of the non-treated WF_sT and of the treated WF_sT with NaOH.

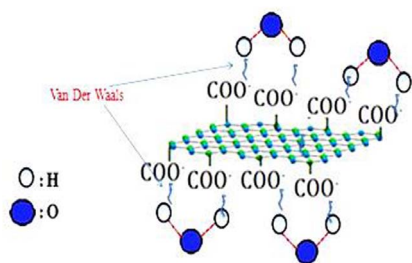


Figure 5. Effect of alkaline treatment on the surface of wood fibers [21].

when the WF_sT are immersed in a basic NaOH solution, the ionization of the hydroxyl group OH can occur on the surface of the fibers (Figure 5).

3.3.2. Infrared spectral characteristics of organoclay

In the FTIR spectra of pure clay and of clay treated with H₂SO₄ and clay modified with CTAB (Figure 6), the band at 3624–3390 cm⁻¹ presented an OH stretching vibration. The treatment of clay with the CTAB led to the appearance of two peaks (2918–2849 cm⁻¹) assigned to the valence variations of the –CH₂ stretching vibration. The bond OH (1633 cm⁻¹) corresponds to water molecules adsorbed on the fiber surface [33] (Figure 6). The important band around 3539 cm⁻¹ during the treatment with sulfuric

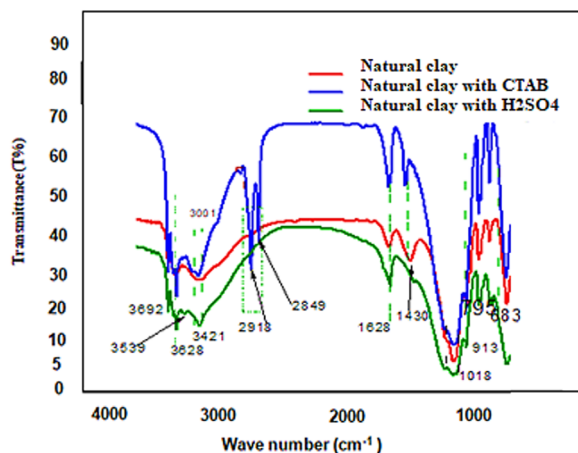


Figure 6. Infrared spectral characteristics of natural clay, natural clay with CTAB and of natural clay treated with H₂SO₄.

acid is attributed to the vibrations of deformations of the H₂O molecules. The band at 3421 cm⁻¹ is attributed to the internal hydroxyls linked to aluminum. Similar results were reported in the literature [29].

In the 2000–500 cm⁻¹ range, the raw and modified clay spectra reveal several characteristic absorption bands. The band at 1018 cm⁻¹ confirms the existence of Si–O–Si bonds in crude clay. We note that the clay is known by the appearance of a peak at 3631 cm⁻¹ and shoulders at 3689 and 3401 cm⁻¹. This peak is

particularly characteristic of clay, and corresponds to stretching vibration of elongation of the OH groups of the octahedral layer band associated to the Si–O–Si stretching vibration of clay. The peaks at 1430 cm^{-1} and 3421 cm^{-1} are attributed to the presence of O–H stretching vibration.

3.4. Contact angle measurements

Contact angle measurements were performed to analyze the relation between the liquid drop and the surface (Figure 7). From these different curves, it is demonstrated that only the natural clay treated with the CTAB allows modifying the character of the composite (cement + fiber) from a hydrophobic character having a high contact angle (in the order of 130) to a hydrophilic character with a low contact angle (in the order of 46). Moreover, the addition of the SDBS in the elaboration of samples makes them more hydrophobic, which is explained by the electrostatic interactions [23].

The non-treated WFs added in the composites have a totally hydrophobic character but the addition of the treated WFs decreases the contact angle more precisely, which decreases the hydrophobicity and confirms that the value of contact angle decreases with the addition of WF-treated and (1 wt%) OC. On the other hand, the addition of SDBS surfactant increases the contact angle, and consequently the hydrophobicity of composites materials.

3.5. Density and porosity

3.5.1. Density

The study of the apparent density for the developed composite materials reinforced clay and fibers is presented in Table 4. The density value was measured by determining the mass and the dimensions of the prepared composites. The results of mixing natural clay and cement with variation of 1%, 2%, 4%, 6%, 8% and 10% of WFsT indicate that the addition of WFsT on C–OC creates porosity inside the composite material which makes it lighter and very practical in comparison with results in the literature [35]. The composite containing WFsT showed a lower density than pure composites. This could be due to the appearance of voids between the interfacial areas of WFsT and of the composite-based cement. For composites with 10 wt% of WFsT, the density decreased

Table 4. The density and the porosity values of WFsT reinforced cement

Samples	Density (kg/m^{-3})	Porosity (%)
Composite	1300	3.99
Composite + 1% WFsT	1190	4.54
Composite + 2% WFsT	1110	2.03
Composite + 4% WFsT	990	1.82
Composite + 6% WFsT	840	3.05
Composite + 8% WFsT	800	4.36
Composite + 10% WFsT	730	3.82

by 43%. This result proves the filling effect of WFsT on the density of cement composites [26]. The density of composite with 10 wt% of WFsT decreased. Such behavior can confirm that WFT reduces density and offers a composite material with a consolidated microstructure.

3.5.2. Porosity

The results of porosity and absorbability values of cement, WFsT reinforced composite and WFsT–OC reinforced composites are shown in Figure 8. The porosity of composite is improved with WFsT inclusion. These results could be assigned to the formation of voids at the interfacial areas between WFsT and composite-based cement. For composites with 2 and 4 wt% of WFsT, the porosity decreased by 1.82% (4 wt% (WFsT)). We conclude that the addition of WFsT has a filling effect on the porosity of composite-based cement. The addition of 2 wt% and 4 wt% of WFsT are able to saturate the surface and to reduce pores. Figure 9 shows that the presence of OC in the composite has reduced the adsorbed water rate of the composite. The optimum percentage of OC was found at 1 wt%. The presence of OC decreased the porosity values of composite by 18.75% with comparison to the cement. This indicates that OC operates in the composite as a pore-filling agent to decrease the porosity values and saturate pores. However, adding less than 1 wt% of OC increased the porosity of all samples due to the agglomeration effect. This result is compared to the cement that is less dense, and contains more pores. Composites with 1 wt% of OC is more compact with few pores, as asserted by the literature [36].

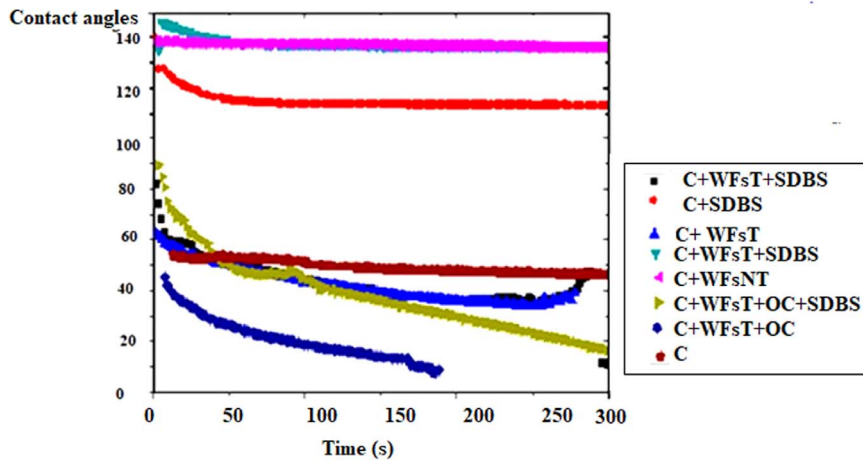


Figure 7. Contact angles measurements.

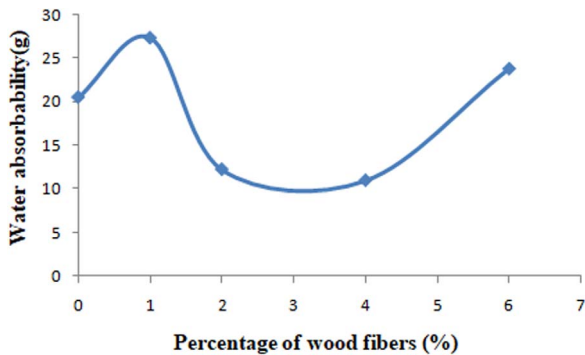


Figure 8. The influence of percentage of wood fiber in the composite on the water absorbability.

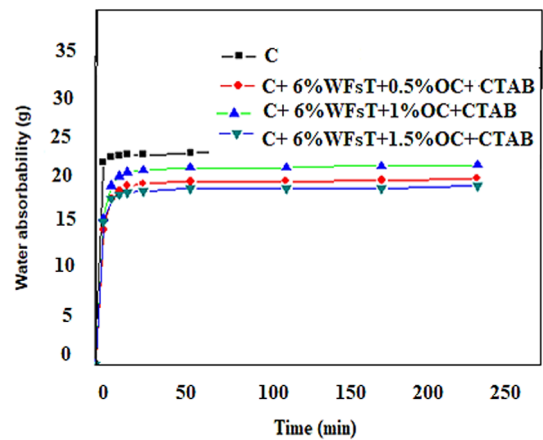


Figure 9. The effect of time on the water absorbability of composite samples.

3.6. Mechanical properties

3.6.1. Compressive strength

Pretreatment of wood fibers with NaOH. The study of compressive strength for WFsT treated with NaOH, and cement composite reinforced by non-treated WFsT are shown in (Figure 10). The effect of WFsT treated by NaOH on the compressive strength of cement composite was evaluated. The results of compressive strength of WFsT-reinforced cement was increased from 9.81 MPa to 18.41 MPa, with about 46.71% rise compared to cement composite reinforced by untreated WFsT. This enhancement is explained as follows: in sequence to enhance the

links between fibers and the OPC, the composite could be modified by reducing or consuming the calcium hydroxide (CH). The low value of the compressive strength might be due to the high sugar and hemicellulose present in fast growing wood. Conversely, chemical treatment led to good mechanical properties [12].

Effect of organoclay. The effects of OC on the compressive strength of 0, 0.5, 1 and 1 wt%. WFsT-cement-composites after 28 days are given in Figure 11. It is clear that the compressive strength value was increased by the addition of OC after 28 days.

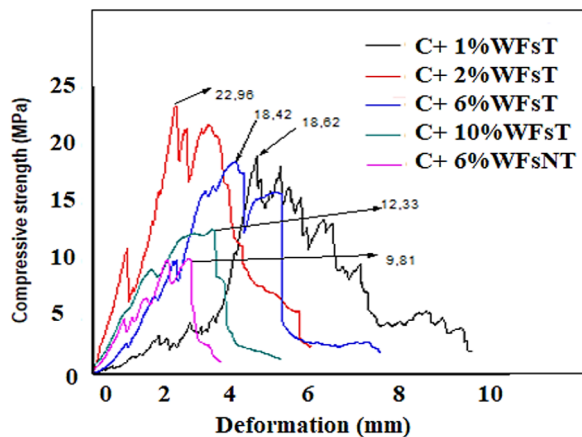


Figure 10. The effect of deformation on the compressive strength.

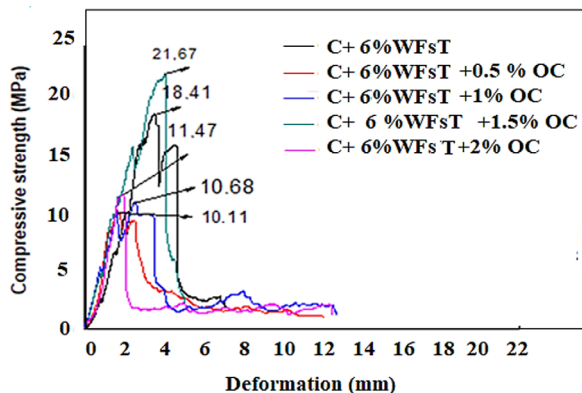


Figure 11. The effect of deformation on compressive strength for the different composites.

After 28 days, the compressive strength of 1 wt% was 21.76 MPa, higher than that of 0.5 wt% of OC (10.11 MPa). The reasons for the enhancement in mechanical properties of composites are as follows. Firstly, the physical effects of 1 wt% of OC, including filling, can reduce the voids or the porosities in the cement matrix, in which the OC was inserted inside the composite-based cement. Thus, it improves the structure and microstructure of composites denser than the WFsT-composite-based cement. Secondly, in the cement matrix, a reaction between OC and calcium hydroxide (CH) produces calcium-silicate-hydrate (C-S-H). Nevertheless, the addition of OC (>1 wt%) led to a decrease in compressive strength. In fact, the compressive strength of 2 wt%

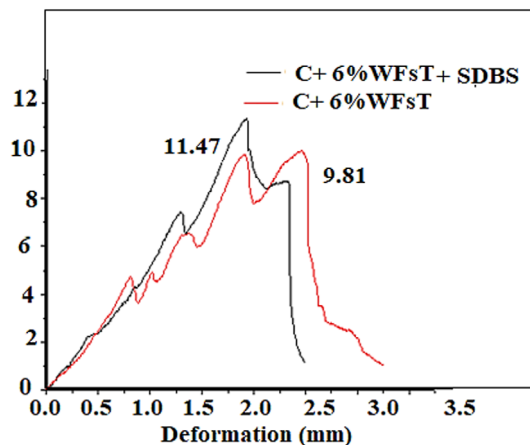


Figure 12. The influence of deformation on compressive strength.

OC was 11.47 MPa. This is due to the bad dispersion and agglomeration of the OC in the composite-based cement at a higher percentage of OC contents, which increases porosity and reduces the link between the fiber and the composite adhesion. In fact, the compressive strength was decreased in the cement-composite with a higher dosage of OC.

Effect of surfactant (SDBS/CTAB). The influence of SDBS on compressive strength of composite materials with non-treated WFsT is described in Figure 12. It shows that the presence of SDBS in composite-based cement increased the compressive strength from 9.81 MPa to 11.47 MPa. About 14.47% improvement can be explained by the adhesion and the collision of fibers in the matrix in the presence of the SDBS [21].

The SDBS has an essential role in the surface packaging of the fiber. It is defined as a super plasticizer that covers the surface of the fibers and renders them hydrophobic. In our case, anionic surfactants are able to agglomerate in the cement to fill the existing pores in the fibers.

Using an anionic surfactant as an adjuvant between the clay platelets treated with CTAB and the cement allows to react with calcium hydroxide $\text{Ca}(\text{OH})_2$ by promoting the formation of additional hydration of the calcium-silica type (CSH) in the form of a gel.

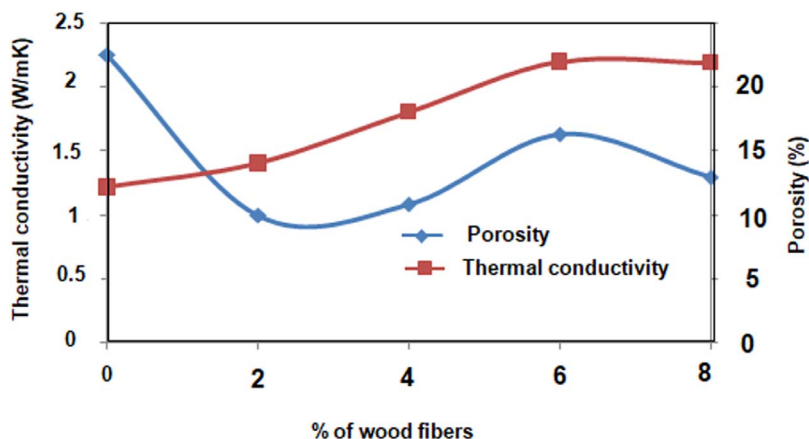


Figure 13. Effect of the percentage of wood fibers on thermal conductivity and porosity.

3.6.2. Thermal conductivity

Thermal conductivity is a very important property of construction and building materials [37]. In this part, the relationship between WFsT contents in composite and thermal conductivity and porosity is studied.

The influence of wood fiber amount. The average thermal conductivities of composite material reinforced with WFsT are 2.26, 1.00, 1.08, 1.63 and 1.09 W/m·K. The mentioned results demonstrate that rising fibers amounts of 0%, 2%, 4%, 6% and 8% W·m⁻¹·K⁻¹, respectively, caused a decreasing thermal conductivity rate to 50% in comparison to the pure composite without WFsT. This reduction may be due to the quantity of WFsT added that is insufficient to favor the establishment of a homogeneous structure. Moreover, the thermal conductivity of a material depends on several parameters such as the nature of the constituent elements of the material, the water content, the temperature and the porosity [38].

The influence of porosity and thermal properties. We examined the relation between the thermal conductivity and the porosity as a function of the percentage of WFsT (Figure 13). In addition, we note that the supplementation of the WFsT in the cement increases the porosity of this material [17,39] (reinforcement by the natural and treated wood). Also, the thermal conductivity results showed a decrease

with the increase of percentage in the WFsT in comparison with the reference sample (Composite). In general, lower values of thermal conductivity were due to the high porosity of the WFs and the large amount of composite materials in the cement. In order to explain the decrease of different percentages of WFs, it can be concluded that 2 wt% of WFsT and 1% of OC contribute to good thermal conductivity of the composites materials compared to the reference sample. Hence, thermal conductivity of the composite increased with further incorporation of wood up to more than 6 wt%. In comparison with hybrid composites (see Figure 13), the reference showed better thermal conductivity results. These obtained results can be explained by the presence of WFsT in the composite [40]. Hence, the surface of the WFsT exhibited the presence of the pores, which may reduce the adhesion of the fibers with cement matrix. The WFsT-OC-matrix adhesion presents a necessity in the overall performance of the composite.

3.7. Interaction between the fibrous suspension modified by surfactant, the cement matrix and the clay

The interactions between the cement, WFs and clay modified by CTAB are summarized in Figures 14 and 15:

- (a) An adsorption of molecules having SO₃²⁻, COO⁻ type functions or a polar function such as OH.

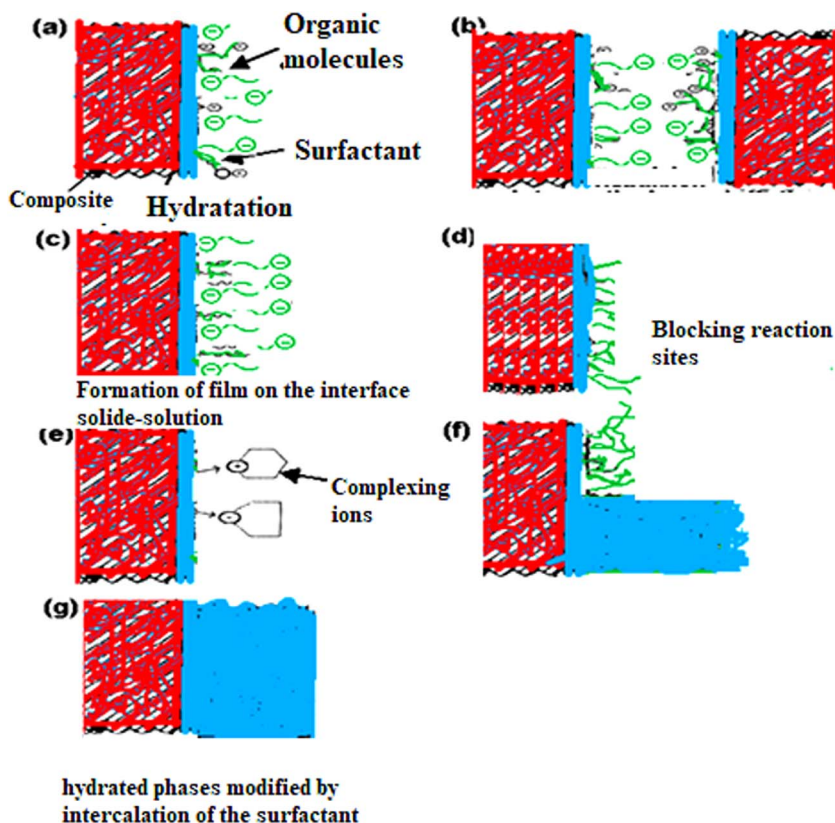


Figure 14. Process describing the interaction between the composite and the surfactant.

- (b) The interaction describes an inter-granular repulsion; particularly due to the case of super plasticizers. It is an adsorption of charged polymers.
- (c) The formation of micelles at the solid-solution interface.
- (d) This mechanism explains the chemisorption of polynaphthalene sulfonate on specific reaction sites, such as these two aluminates.
- (e) This figure proposes the action of sugars or hydroxyl carboxylic acids by complexation in the interstitial solution. This complexation can then delay the precipitation of hydrates such as portlandite or C-S-H.
- (f) The mechanism (f) suggests that the CTAB surfactant plays the role of potentially inhibiting the growth of hydrates by adsorbing on specific crystallographic growth sites.
- (g) The figure (g) describes the insertion of the polymer into the structure of the hydrate.

4. Conclusion

In this paper, the enhancement and the testing of the properties of composite containing C-WFsT-OC were investigated. In particular, the effect of WFsT inclusion on the thermal, mechanical and physical properties of this type of material was evaluated.

The mechanical properties of this study showed that the optimum content of OC and WFsT in the composite is 1 wt% and 6 wt%, respectively. The thermal conductivity of cement composites could be enhanced by the addition of 2 wt% of treated WFs and 1 wt% of OC.

Due to the hydrophilic nature of WFsT, a reduction in porosity (15.78%) and density, the enhancement in compressive strength (18.11%) and the decrease of thermal conductivity are ameliorated by the addition of 1 wt% of OC. Moreover, introducing OC treated by the CTAB and WFs into cement matrix could lead

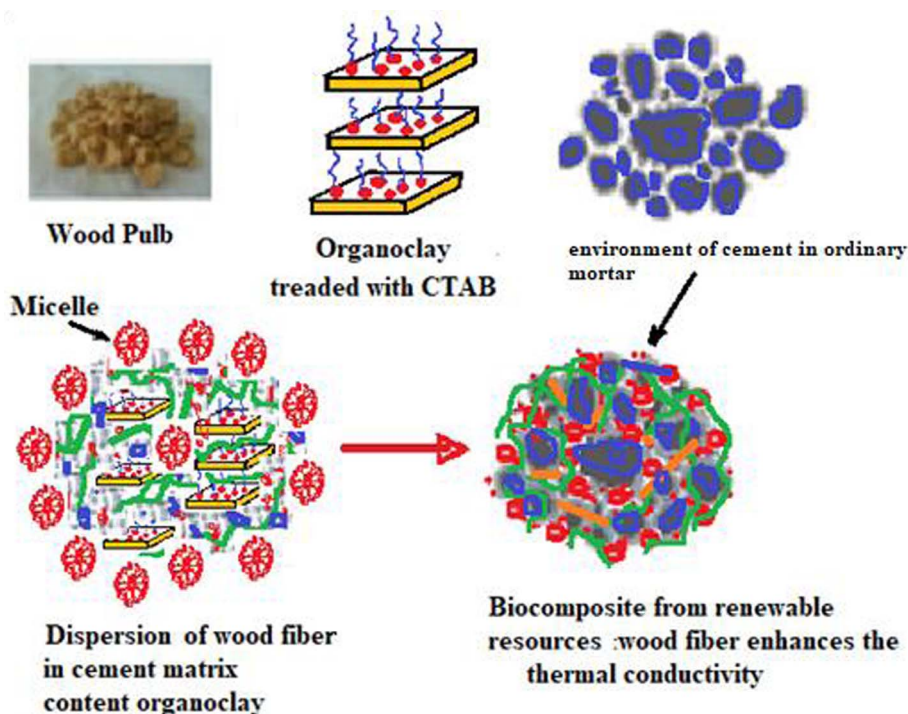


Figure 15. Dispersion of WF and state of the environment of cement grains.

to accelerate hydration and to reduce the thermal conductivity to ensure a good insulation.

Notation

C = Cement
 CTAB = Cetyltrimethylammonium bromide
 CSH = Calcium–silica–hydration
 NaOH = Sodium hydroxide
 OPC = Ordinary Portland cement NF P 15-301
 OC = Organoclay
 SDBS = Sodium dodecylbenzene sulfonate
 WFsT = Wood fibers treated
 WFsNT = Wood fiber non-Treated

Acknowledgments

Authors are grateful to the Laboratory of Energy and Materials (LABEM) for the financial support of this work and would also like to express their gratitude to the FP7 FP4BATIW Euro-Mediterranean project.

References

- [1] M. Boumhaout, L. Boukhattem, H. Hamdi *et al.*, *Constr. Build. Mater.*, 2017, **135**, 241-250.
- [2] A. Sadeghi-nik, J. Berenjian, A. Bahari *et al.*, *Constr. Build. Mater.*, 2017, **155**, 880-891.
- [3] R. Chihi, I. Blidi, M. Trabelsi-Ayadi, F. Ayari, *C. R. Chim.*, 2019, **22**, 188-197.
- [4] R. Guégan, *C. R. Chim.*, 2019, **22**, 132-141.
- [5] R. Demirbog, *Constr. Build. Mater.*, 2017, **156**, 208-218.
- [6] A. Hakamy, F. U. A. Shaikh, I. M. Low, *Cement Concrete Composites*, 2014, **50**, 27-35.
- [7] A. Folli, I. Pochard, A. Nonat *et al.*, *J. Am. Ceram. Soc.*, 2010, **93**, 3360-3369.
- [8] J. Leitner, V. Barůtněk, D. Sedmidubský, O. Jankovský, *App. Mater. Today*, 2018, **10**, 1-11.
- [9] H. Assaedi, F. U. A. Shaikh, I. M. Low, *J. Asian Ceram. Soc.*, 2017, **5**, 62-70.
- [10] J. Wei, S. Ma, D. G. Thomas, *Corros. Sci.*, 2016, **106**, 1-15.
- [11] J. Claramunt, R. Dias, T. Filho, *Constr. Build. Mater.*, 2015, **79**, 115-128.
- [12] J. Calabria-holley, S. Papatzani, B. Naden *et al.*, *Appl. Clay Sci.*, 2017, **143**, 67-75.
- [13] Y. Sun, P. Gao, F. Geng *et al.*, *Mater. Lett.*, 2017, **209**, 349-352.
- [14] A. Rahman, Y. C. Ching, K. Y. Ching *et al.*, *BioResources*, 2015, **10**, 7405-7418.
- [15] N. Hamdi, I. Ben Messaoud, E. Srasra, *C. R. Chim.*, 2019, **22**, 220-226.

- [16] B. Feneuil, O. Pitois, N. Roussel, *Cement Concrete Res.*, 2017, **100**, 32-39.
- [17] J. Calabria-Holley, S. Papatzani, B. Naden *et al.*, *Appl. Clay Sci.*, 2017, **143**, 67-75.
- [18] R. Cioffi, L. Maffucci, L. Santoro, F. P. Glasser, *Waste Manage.*, 2001, **21**, 651-660.
- [19] S. H. Ghaffar, *Straw Fibre-Based Construction Materials*, Elsevier Ltd, 2016.
- [20] Z. Grigale-Sorocina, I. Birks, *C. R. Chim.*, 2019, **22**, 169-174.
- [21] F. Aloulou, S. Alila, H. Sammouda, *J. Renew. Mater.*, 2019, **7**, 763-774.
- [22] TAPPI, *TAPPI Standards: Regulations and Style Guidelines*, TAPPI Publications, 2018.
- [23] A. Fadhel, A. Sabrine, *Int. J. Ind. Chem.*, 2018, **9**, 265-276.
- [24] A. Mishra, J. Hanley, D. B. Tripathy, J. Clark, T. Farmer, "Synthesis, chemistry, physicochemical properties and industrial applications of amino acid surfactants: A review", This is a repository copy of White Rose Research Online URL for this paper at <http://eprints.whiterose.ac.uk/133786>. Accepted version available in *Comptes Rendus Chimie* journal, 2018.
- [25] G. B. Kankiliç, A. Ü. Metin, I. Tüzün, *Ecol. Eng.*, 2016, **86**, 85-94.
- [26] A. Hakamy, F. U. A. Shaikh, I. Low, *Cement Concrete Compos.*, 2014, **50**, 27-35.
- [27] F. Aloulou, S. Alila, *J. Renew. Mater.*, 2019, **7**, 557-566.
- [28] H. Bel Hadjtaief, S. Ben Ameer, P. Da Costa *et al.*, *Appl. Clay Sci.*, 2018, **152**, 148-157.
- [29] T. C. D. C. Costa, J. D. D. Melo, C. A. Paskocimas, *Ceram. Int.*, 2013, **39**, 5063-5067.
- [30] I. Fatimah, *J. Mater. Environ. Sci.*, 2012, **3**, 983-992.
- [31] C. W. Foley, J. Seitzman, T. Lieuwen, "Blowoff scaling of bluff body stabilized flames", in *Fall Technical Meeting of the Eastern States Section of the Combustion Institute 2011*, vol. 45, Combustion Institute, 2011, 606-614.
- [32] G. Goncalves, P. A. A. P. Marques, R. J. B. Pinto *et al.*, *Compos. Sci. Technol.*, 2009, **69**, 1051-1056.
- [33] S. S. Bhattacharya, M. Aadhar, *Res. J. Eng. Sci.*, 2014, **3**, 10-16.
- [34] A. Fadhel, A. Sabrine, *Int. J. Ind. Chem.*, 2018, **9**, 265-276.
- [35] D. v. Westen, G. Skagerberg, J. Olsrud, P. Fransson, E.-M. Larsson, *Acta Radiol.*, 2005, **46**, no. 6, 599-609.
- [36] H. El-Sokkary, K. Galal, *J. Compos. Constr.*, 2019, **23**, article no. 04019032.
- [37] M. Ge, C. Cao, J. Huang *et al.*, *J. Mater. Chem. A*, 2016, **18**, 6772-6801.
- [38] J. Huo, Z. Peng, Q. Feng *et al.*, *Solar Energy*, 2018, **169**, 84-93.
- [39] S. Pilehvar, V. Duy, A. M. Szczotok *et al.*, *Cement Concrete Res.*, 2017, **100**, 341-349.
- [40] F. Balo, L. S. Sua, *Int. J. Appl. Ceramic Technol.*, 2018, **15**, 792-814.